Christopher Church
Junjie Zhu
Xiangchun Xuan

Department of Mechanical Engineering, Clemson University, Clemson, SC, USA

Received July 28, 2010
Revised October 4, 2010
Accepted October 18, 2010

Research Article

Negative dielectrophoresis-based particle separation by size in a serpentine microchannel

Dielectrophoresis has been widely used to focus, trap, concentrate, and sort particles in microfluidic devices. This work demonstrates a continuous separation of particles by size in a serpentine microchannel using negative dielectrophoresis. Depending on the magnitude of the turn-induced dielectrophoretic force, particles travelling electrokinetically through a serpentine channel either migrate toward the centerline or bounce between the two sidewalls. These distinctive focusing and bouncing phenomena are utilized to implement a dielectrophoretic separation of 1 and 3 μm polystyrene particles under a DC-biased AC electric field of 880 V/cm on average. The particle separation process in the entire microchannel is simulated by a numerical model.

Keywords:
Dielectrophoresis / Electrokinetic flow / Microfluidics / Particle separation / Serpentine microchannel
DOI 10.1002/elps.201000396

1 Introduction

Dielectrophoresis (DEP) is a powerful tool for particle focusing, trapping, concentration, and separation in microfluidic devices [1–3]. It has been realized using both electrode- [4, 5] and insulator-based [6, 7] approaches. Electrode-based DEP uses the non-uniform AC electric field between electrodes that are placed inside a microchannel to generate the dielectrophoretic force for particle manipulation [8–11]. Difficulties with this method include increased fabrication complexity and electrode fouling [12]. Insulator-based DEP eliminates these difficulties by using in-channel insulators like hurdles, posts, and ridges to generate the non-uniform AC or DC field [13, 14], which is applied through electrodes virtually outside the microchannel. This technique has been demonstrated by various research groups to align, enrich, and sort particles and cells in microfluidic devices [15–22]. However, the in-channel micro-obstacles may cause adverse effects on the sample and device due to Joule heating and particle clogging, etc. [23]. These issues are mitigated when the channel curvature is utilized to generate DEP [24–27].

The authors have recently demonstrated a continuous dielectrophoretic separation of particles in a double-spiral microchannel [28]. Due to the curvature-induced negative DEP, particles are focused to a stream flowing near the outer wall of the first spiral, and then deflected toward different flow paths in the second spiral, enabling a size-based sorting. In another study, the authors combined the negative and positive dielectrophoretic focusing phenomena to implement a particle separation in a serpentine microchannel [29]. This happens because the larger particles experience negative DEP and migrate to the channel centerline while the smaller particles undergo positive DEP and line the sidewalls of the serpentine channel. In the present work, we demonstrate a continuous particle separation in a serpentine microchannel using negative dielectrophoretic focusing and bouncing effects. This is because small particles migrate toward the channel centerline while large particles bounce between the two sidewalls due to the particle volume dependence of the dielectrophoretic force induced within the channel turns.

2 Materials and methods

The serpentine microchannel was fabricated with polydimethylsiloxane (PDMS) using the standard soft lithography method, and was rendered hydrophilic through plasma treating. Detailed information on this procedure is referred to Church et al. [25]. As shown in Fig. 1, the microchannel consists of a 1-cm-long serpentine section (with totally 33 periods) for focusing particles followed by a T-junction for sorting the particles. It has a uniform width and depth of 50 and 15 μm, respectively, with one inlet and two outlet

Correspondence: Professor Xiangchun Xuan, Department of Mechanical Engineering, Clemson University, Clemson, SC 29634-0921, USA
E-mail: xcxuan@clemson.edu
Fax: +1-864-656-7299

Abbreviations: CM, Clausius–Mossotti; **DEP,** dielectrophoresis; **RMS,** root-mean-square

Colour Online: See the article online to view Figs. 1–4 in colour.

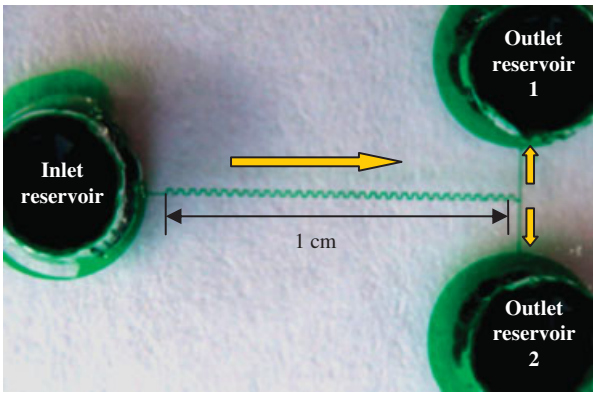

Figure 1. Picture of the serpentine microchannel with the block arrows indicating the flow directions in the separation experiment.

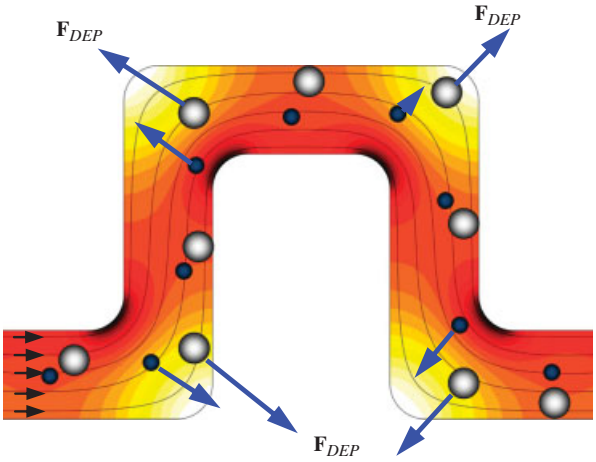

Figure 2. Illustration of the mechanism for the negative DEP-based particle separation in a serpentine microchannel (only one period is shown) where small particles (dark shaded circles) are focused to the centerline while large particles (light shaded circles) are bounced between the two sidewalls. The background shows the electric field contour (the darker the higher) and electric field lines in the absence of particles. The approximate magnitude of the turn-induced dielectrophoretic force on a particle, $\mathbf{F}_{DEP}$, is indicated by the length of the vector.

reservoirs attached to the ends. For the demonstration of particle separation, 1-μm-diameter fluorescent polystyrene particles (FS04F, dragon green with 480/520 nm for the excitation/emission wavelengths, Bangs Laboratories) and 3-μm-diameter plain polystyrene particles (17134, Polysciences) were mixed and re-suspended in 1 mM phosphate buffer (pH 7) to a concentration of about 10^7 particles/mL for each. Tween 20 (0.5% v/v, Sigma-Aldrich) was added to the suspension for suppressing particle aggregations and adhesions to the channel walls. The DC-biased AC voltages were supplied using a function generator (33220A, Agilent Technologies) with a high-voltage amplifier (609E-6, Trek). The frequency of AC voltages was fixed at 1 kHz, and was found to have little influence on particle motion in the frequency range of the amplifier (up to 6 kHz for large voltages). Particle motion was visualized and recorded through an inverted microscope (Eclipse TE2000U, Nikon Instruments) equipped with a CCD camera (Nikon DS-Qi1Mc).

3 Theory

Figure 2 shows the electric field contour (the darker the higher) and the electric field lines in the absence of particles within one period of the serpentine section. Due to the channel curvature, the electric field becomes spatially non-uniform creating a local maximum and minimum at the inner and outer corners of each 90° turn. As a result, particles moving electrokinetically through the channel experience a cross-stream dielectrophoretic force, whose time-average, $\mathbf{F}_{DEP}$, in DC and low-frequency AC electric fields is expressed as [30]

$$\mathbf{F}_{DEP} = (1/2)\pi\varepsilon_f d^3 f_{CM}(\mathbf{E}\cdot\nabla\mathbf{E}) \quad (1)$$

$$f_{CM} = (\sigma_p - \sigma_f)/\sigma_p + 2\sigma_f \quad (2)$$

where ε_f is the permittivity of the suspending fluid, d the particle diameter, f_{CM} the so-called Clausius–Mossotti (CM) factor that has been assumed to remain unvaried in DC and low-frequency AC fields [12, 31], $\mathbf{E}$ the root-mean-square (RMS) electric field, σ_p the electric conductivity of the particle, and σ_f is the electric conductivity of the fluid. Note that f_{CM} in Eq. (2) is determined solely by the electric conductivity difference between the particle and solution for DC and low-frequency AC fields. In contrast, f_{CM} in electrode-based DEP is generally dependent on the differences in both the conductivity and the permittivity of the particle and solution as high-frequency AC fields are employed.

As the polystyrene particles used in the experiment [32] (and live biological cells [33] as well) are less conductive than the buffer solution, f_{CM} becomes negative yielding negative DEP. This results in particle deflection toward the outer corner of each turn where the electric field is the lowest. Therefore, particles should be gradually focused to the channel centerline as demonstrated previously [24, 25, 29]. However, in the situation where the DEP force is too strong due to, for example, a very high electric field [24] or a DC-biased AC electric field [25, 29], particles can be deflected past the centerline to the outer wall of each turn. This will force the particles to bounce between the two sidewalls and flow out of the serpentine section near one sidewall. As the DEP force is proportional to the particle volume, see Eq. (1), it is likely to use these distinctive focusing (to the centerline) and bouncing (to the sidewall) effects in a serpentine microchannel to separate particles by size.

In order to simulate the focusing and bouncing effects of negative DEP on particle separation, a numerical model was developed to simulate the electrokinetic particle transport in the serpentine microchannel. This model, originally developed by Kang et al. [34], ignores the perturbations of

particles on the flow and electric fields. Rather, a correction factor, c, was introduced to account for the particle size and wall effects on the dielectrophoretic velocity. This model has been validated by the authors through comparisons with several experiments [18, 24–26, 29, 35]. In this model, the particle velocity, $\mathbf{U}_p$, is given by

$$\mathbf{U}_p = \mu_{EK}\mathbf{E}_{DC} + c\mu_{DEP}(\mathbf{E}\cdot\nabla\mathbf{E}) \quad (3)$$

$$\mu_{DEP} = \varepsilon_f d^2 f_{CM}/6\mu_f \quad (4)$$

where μ_{EK} is the particle mobility of DC electrokinetic motion (a combination of fluid electroosmosis and particle electrophoresis), $\mathbf{E}_{DC}$ the DC component of the applied RMS electric field $\mathbf{E}$, and μ_{DEP} the dielectrophoretic particle mobility with μ_f being the fluid dynamic viscosity. Note that both fluid and particle inertia have been neglected in Eq. (3) considering the flow's low Reynolds and Dean numbers in the serpentine microchannel. In addition, Joule heating effects and turn-induced pressure-driven flow are negligible in the experimental conditions.

The numerical modeling was carried out using COMSOL® (Burlington, MA), and the detail is referred to Church et al. [25, 29]. The electrokinetic mobility, μ_{EK}, was determined by tracking the motion of individual 1 and 3 μm particles in the straight channel between the two outlet reservoirs (see Fig. 1) during the separation experiment, and was found to be $3.5\times10^{-8}\,m^2/(V\,s)$ on average for both particles. Their electric conductivities were calculated as 40 and 13.3 μS/cm, respectively, if the surface conductance is assumed to be 1 nS [24, 25, 32]. As the measured electric conductivity of the buffer solution is 210 μS/cm, the CM factors, f_{CM}, were determined as −0.37 and −0.45 for 1 and 3 μm particles, respectively. Their correction factors, c, were both set to 1.0 and 0.8, consistent with previous studies [24–26, 29].

4 Results and discussion

Figure 3 shows the experimentally obtained (top) and numerically predicted (bottom) trajectories of 3 μm plain particles (dark) and 1 μm fluorescent particles (green) at the entrance to the serpentine section of the microchannel. The applied DC-biased AC voltages are 1600 V at the inlet reservoir, 0 V at the outlet reservoir 1, and 10 V at the outlet reservoir 2 (refer to Fig. 1). The AC to DC voltage ratio is 15:1, corresponding to 1500 V RMS AC and 100 V DC. The average RMS electric field in the serpentine section of the microchannel is about 880 V/cm as determined from the numerical modeling. The measured particle velocity in the serpentine section is around 160 μm/s. The electric current was monitored and found to remain constant for over 5 min without a noticeable change. This indicates negligible Joule heating effects during the separation experiment [36].

Due to the curvature-induced negative DEP, 1 μm particles began to be focused within the first few turns of the serpentine section as seen in Fig. 3 (top). In contrast, 3 μm particles entered into the serpentine section in an already focused stream along the channel centerline. This happened mainly due to the wall-induced lateral migration as demonstrated recently by Liang et al. [37]. Moreover, since they experienced a much larger dielectrophoretic force than 1 μm particles, 3 μm particles were deflected past the channel centerline to the outer sidewall. This occurred each time they passed a channel turn at its inner corner as illustrated in Fig. 3. The experimentally observed focusing and bouncing behaviors (top) of the two particles agree reasonably with the numerically predicted particle trajectories (bottom).

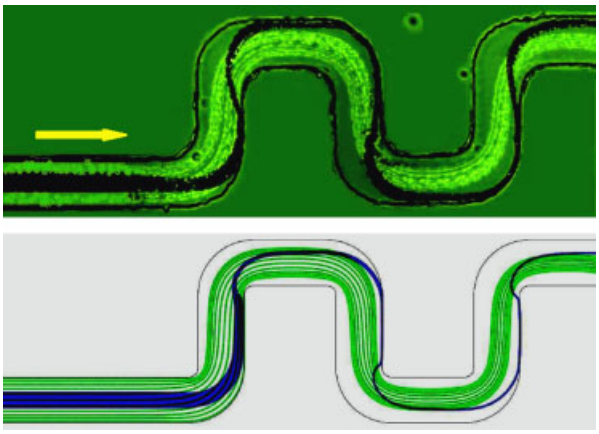

Figure 3. Trajectories of 3 μm plain particles (dark) and 1 μm fluorescent particles (green) at the entrance to the serpentine section of the microchannel illustrating the distinctive focusing and bouncing effects: top from experiment and bottom from modeling. The applied total electrical field is 880 V/cm with the AC to DC field ratio being 15. The block arrow indicates the flow direction.

Figure 4 shows the experimentally obtained (top) and numerically predicted (bottom) trajectories of 3 μm particles (dark) and 1 μm particles (green) at the exit to the serpentine section of the microchannel, i.e. at the T-junction. The simulation once again agrees reasonably well with the experimental results. As seen from the figure, 1 μm particles were nicely focused by negative DEP to the channel centerline after exiting the serpentine section of the microchannel. However, the measured stream width of about 8 μm is much larger than the numerical prediction. The possible reason for this deviation will be discussed shortly. In the meantime, due to the DEP-induced bouncing effect, 3 μm particles were deflected to the outer wall in a well-focused stream with the width being nearly the particle diameter as they moved past the last turn at the exit of the serpentine section. The difference in the final positions of these two particles allows for a continuous separation at the T-junction of the microchannel. Specifically, 1 μm particles were observed moving to the top branch of the junction (i.e. toward outlet reservoir 1, refer to Fig. 1) while 3 μm particles took the lower branch (i.e. toward outlet reservoir 2). It is important to note that the dielectrophoretic focusing of 1 μm particles to the channel center is necessary for the

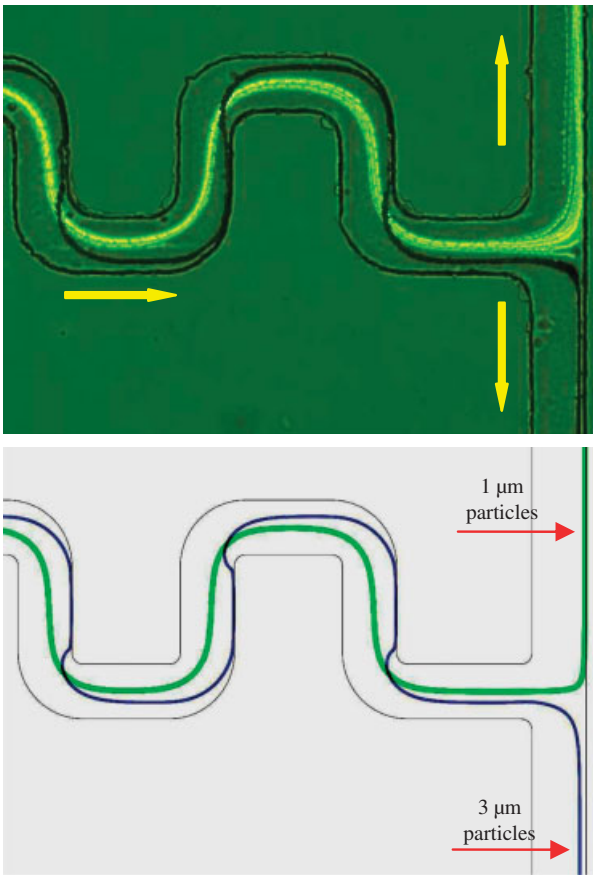

Figure 4. Trajectories of 3 μm plain particles (dark, go downward) and 1 μm fluorescent particles (green, go upward) at the exit to the serpentine section of the microchannel (i.e. the T-junction) illustrating a size-based continuous separation: top from experiment and bottom from modeling. The applied total electrical field is 880 V/cm with the AC to DC field ratio being 15. The block arrows indicate the flow directions.

demonstrated separation. This focusing depends on both the applied electric field (also responsible for the dielectrophoretic bouncing of 3 μm particles) and the number of serpentine periods.

During the separation, 1 μm particles were occasionally observed to flow with 3 μm particles into the lower branch of the separation junction, which is not clearly shown in Fig. 4. This incomplete separation (though still >90% purity as confirmed by the post-separation counting of the two particles in the two reservoirs) is believed to be associated with three issues: (i) there exists a small stagnation region at the T-junction (see the near-wall area in between the two sorted particle streams in Fig. 4), where the local electric field and flow velocity are close to zero so that the Brownian motion may affect the travelling direction of 1 μm particles; (ii) there is an unavoidable inhomogeneity in the particle size and properties (e.g. surface charge) due to fabrication defects, which causes a small number of 1 μm particles not to be well focused; (iii) there occurs a pressure drop in the channel between the two outlet reservoirs (see Fig. 1) due to the uneven distribution of the flow rate at the T-junction.

As the numerically predicted particle trajectories agree reasonably with the experimental results in Figs. 3 and 4, the current model was also used to examine the potential and limits of the demonstrated particle separation technique. If the applied DC voltage is fixed at 100 V, a minimum of 900 V AC is required to ensure that 3 μm particles can still go past the centerline and be separated from 1 μm particles in the fabricated serpentine microchannel (note: the average electric field is 550 V/cm in the serpentine section). Moreover, the AC voltage must not be higher than 2400 V, otherwise, both sizes of particles will bounce between the two sidewalls and cannot be separated. Additionally, the minimum size difference of the particles that can be sorted was numerically studied under the conditions identical to the above experiment. It was found that particles with diameter down to 1.8 μm can still be separated from 1 μm particles. In contrast, 3 μm particles can at most be separated from particles with a diameter no larger than 1.5 μm. It is important to note that all the numbers presented here are from the numerical modeling, which may differ significantly from the actual experiments. For example, the numerically predicted focusing of 1 μm particles is much better than that obtained from the experiment (see Fig. 4), which has been discussed above.

5 Concluding remarks

A continuous particle separation by size has been demonstrated in a serpentine microchannel using dielectrophoretic focusing and bouncing effects. Both effects arise from the particle deflection caused by the cross-stream negative DEP within the channel turns. Owing to the dependence of the dielectrophoretic force on particle volume, smaller particles are focused to the centerline while larger particles bounce between the two sidewalls allowing for the separation in a serpentine channel. The developed dielectrophoretic separation technique may potentially be used to separate bioparticles with distinct sizes or electrical properties.

This work was supported by NSF under Grant CBET-0853873 and the Clemson University Creative Inquiry Program.

The authors have declared no conflict of interest.

6 References

[1] Velev, O. D., Bhatt, K. H., *Soft Matt.* 2006, *2*, 738–750.

[2] Lapizco-Encinas, B. H., Rito-Palmomares, M., *Electrophoresis* 2007, *28*, 4521–4538.

[3] Xuan, X., Zhu, J., Church, C., *Microfluid. Nanofluidics* 2010, *9*, 1–16.

[4] Gascoyne, P. R. C., Vykoukal, J., *Electrophoresis* 2002, *23*, 1973–1983.

[5] Hughes, M. P., *Electrophoresis* 2002, *23*, 2569–2582.

[6] Chou, C., Zenhausern, F., *IEEE Eng. Med. Biol. Mag.* 2003, *22*, 62–67.

[7] Cummings, E. B., *IEEE Eng. Med. Biol. Mag.* 2003, *22*, 75–84.

[8] Wang, L., Lu, J., Marchenko, S. A., Monuki, E. S., Flanagan, L. A., Lee, A. P., *Electrophoresis* 2009, *30*, 1–10.

[9] Meighan, M. M., Staton, S. J. R., Hayes, M. A., *Electrophoresis* 2009, *30*, 852–865.

[10] Khoshmanesh, K., Zhang, C., Tovar-Lopez, F. J., Nahavandi, S., Baratachi, S., Kalantar-Zadeh, K., Mitchell, A., *Electrophoresis* 2009, *30*, 3707–3717.

[11] Lewpiriyawong, N., Yang, C., Lam, Y. C., *Electrophoresis* 2010, *31*, 2622–2631.

[12] Voldman, J., *Annu. Rev. Biomed. Eng.* 2006, *8*, 425–454.

[13] Chou, C. F., Zenhausern, F., *IEEE Eng. Med. Biol. Mag.* 2003, *22*, 62–67.

[14] Cummings, E. B., *IEEE Eng. Med. Biol. Mag.* 2003, *22*, 75–84.

[15] Lapizco-Encinas, B. H., Simmons, B. A., Cummings, E. B., Fintschenko, Y., *Electrophoresis* 2004, *25*, 1695–1704.

[16] Barrett, L. M., Skulan, A. J., Singh, A. K., Cummings, E. B., Fiechtner, G. J., *Anal. Chem.* 2005, *77*, 6798–6804.

[17] Kang, K., Kang, Y., Xuan, X., Li, D., *Electrophoresis* 2006, *27*, 694–702.

[18] Pysher, M. D., *Anal. Chem.* 2007, *79*, 4552–4557.

[19] Hawkins, B. G., Smith, A. E., Syed, Y. A., Kirby, B. J., *Anal. Chem.* 2007, *79*, 7291–7300.

[20] Kang, Y., Li, D., Kalams, S. A., Eid, J. E., *Biomed. Microdev.* 2008, *10*, 243–249.

[21] Lewpiriyawong, N., Yang, C., Lam, Y. C., *Biomicrofluidics* 2008, *2*, 034105.

[22] Chen, K., Pacheco, J. R., Hayes, M. A., Staton, S. J. R., *Electrophoresis* 2009, *30*, 1441–1448.

[23] Simmons, B. A., Cummings, E. B., Davalos, R. V., Fiechtner, G. J., Lapizco-Encinas, B. H., McGraw, G. J., Salmi, A. J., Ceremuga, J. T., Kanouff, M., Fintschenko, Y., *Separation and concentration of water-borne contaminants utilizing insulator-based dielectrophoresis,* SAND2006-0654, Technical Report, Sandia National Laboratories, 2006, USA.

[24] Zhu, J., Tzeng, T. R., Hu, G., Xuan, X., *Microfluid. Nanofluidics* 2009, *7*, 751–756.

[25] Church, C., Zhu, J., Wang, G., Tzeng, T. J., Xuan, X., *Biomicrofluidics* 2009, *3*, 044109.

[26] Zhu, J., Xuan, X., *J. Colloid Interface Sci.* 2009, *340*, 285–290.

[27] Ai, Y., Park, S., Zhu, J., Xuan, X., Beskok, A., Qian, S., *Langmuir* 2010, *26*, 2937–2944.

[28] Zhu, J., Tzeng, T. R., Xuan, X., *Electrophoresis* 2010, *31*, 1382–1388.

[29] Church, C., Zhu, J., Nieto, J., Keten, G., Ibarra, E., Xuan, X., *J. Micromech. Microeng.* 2010, *20*, 065011.

[30] Morgan, H., Green, N. G., *AC Electrokinetics: Colloids and Nanoparticles*, Research Studies Press, Hertfordshire, UK 2002.

[31] Cummings, E. B., Singh, A. K., *Anal. Chem.* 2003, *75*, 4724–4731.

[32] Ermolina, I., Morgan, H., *J. Colloid. Interface Sci.* 2005, *285*, 419–428.

[33] Pethig, R., Markx, G. H., *Trends Biotechnol.* 1997, *15*, 426–432.

[34] Kang, K., Xuan, X., Kang, Y., Li, D., *J. Appl. Phys.* 2006, *99*, 064702.

[35] Zhu, J., Xuan, X., *Electrophoresis* 2009, *30*, 2668–2675.

[36] Xuan, X., *Electrophoresis* 2008, *29*, 33–43.

[37] Liang, L., Ai, Y., Zhu, J., Qian, S., Xuan, X., *J. Colloid. Interface Sci.* 2010, *347*, 142–146.

